DENTAL MATERIALS 35 (2019) e175–e183

Available online at www.sciencedirect.com

ScienceDirect

journal homepage: www.intl.elsevierhealth.com/journals/dema

Experimental composites containing quaternary ammonium methacrylates reduce demineralization at enamel-restoration margins after cariogenic challenge

André Coimbra Maia[a], Adrielle Mangabeira[b], Renato Vieira[a], Aline de Almeida Neves[b], Ricardo Tadeu Lopes[c], Thais Maria Pires[c], Gil Mendes Viana[d], Lúcio Mendes Cabral[d], Larissa Maria Cavalcante[a,e], Maristela Barbosa Portela[a,*]

[a] Faculdade de Odontologia, Universidade Federal Fluminense, Niterói, RJ, Brazil
[b] Faculdade de Odontologia, Universidade Federal do Rio de Janeiro, Rio de Janeiro, RJ, Brazil
[c] Laboratório de Instrumentação Nuclear, Universidade Federal do Rio de Janeiro, Rio de Janeiro, RJ, Brazil
[d] Faculdade de Farmácia, Laboratório TIF, Universidade Federal do Rio de Janeiro - UFRJ, Rio de Janeiro, RJ, Brazil
[e] Núcleo de Pesquisa em Biomateriais Dentários, Faculdade de Odontologia, Universidade Veiga de Almeida - UVA, Rio de Janeiro, RJ, Brazil

ARTICLE INFO

Keywords:
Dental composite
Quaternary ammonium
Restorative dentistry
Streptococcus mutans
Demineralized enamel
Biofilm

ABSTRACT

Objective. This study evaluated the influence of experimental composites containing quaternary ammonium monomers (QAM) at different concentrations and alkyl chains on demineralization at enamel-composite margins after cariogenic challenge.

Methods. Standardized 4 × 4 mm cavities were cut into 35 bovine enamel blocks, which were randomly divided into seven groups (n = 5) and restored with the following experimental composites and commercial materials: (G12.5) – 5% dimethylaminododecyl methacrylate (DMADDM) with a 12-carbon alkyl chain (G12.10) – 10% DMADDM, (G16.5) – 5% dimethylaminohexadecyl methacrylate (DMAHDM) with a 16-carbon alkyl chain (G16.10) – 10% DMAHDM, (CG) – control group (without QAM), (GZ250) – commercial composite (Filtek Z250®), and (GIC) – glass ionomer cement (Maxxion R®). After restorative procedures, initial microhardness was measured and experimental composites were subjected to *Streptococcus mutans* biofilm formation for 48 h. After cariogenic challenge, the samples were washed and microhardness was reassessed. A 3D non-contact profilometer was used to determine surface roughness and enamel demineralization was assessed by micro-CT. Microhardness results were analyzed by the Kruskal–Wallis and Mann-Whitney tests and micro-CT results were analyzed by Tukey's HSD test (95% confidence interval).

Results. None of the materials could prevent mineral loss at the enamel-restoration margins. The addition of 10% DMAHDM yielded the lowest, albeit statistically significant, mineral loss ($p < 0.05$). 3D non-contact profilometry showed enamel surface roughness modification

* *Corresponding author at*: Faculdade de Odontologia, Departamento de Odontoclínica (MOC), Universidade Federal Fluminense, Rua Mario Santos Braga, 28, Campus do Valonguinho, Centro Niterói, RJ, CEP: 24020-140, Brazil.
E-mail address: mbportela@hotmail.com (M.B. Portela).
https://doi.org/10.1016/j.dental.2019.05.021

after biofilm exposure. The CG had the highest roughness values. Micro-CT analysis revealed mineral loss, except for GIC.

Significance. The addition of 10% QAM with a 16-carbon chain in experimental composites reduced mineral loss at the enamel-restoration margins after cariogenic challenge.

1. Introduction

Although composites are widely used as direct filling materials for tooth restorations, they tend to accumulate more biofilms than any other restorative materials *in vivo* [1]. As a result, biofilms at the enamel or dentin-composite margins may produce acids and cause secondary caries, which is one of the main reasons for restoration failure and replacement [1]. In order to minimize these effects, current research has focused on incorporation of antibacterial monomers into the organic matrix of composites [2,3].

Caries disease is a biofilm-dependent condition in which *Streptococcus mutans* is the main etiologic agent. Dental biofilm is composed of different microorganisms that organize themselves into complex tangles, becoming more pathogenic [4]. The development of caries around a previously restored tooth is related to the progressive demineralization at the tooth-composite interface caused by the acid produced by the adhered biofilm [5–7]. Although composites are the first choice for the restoration of cavities, they cannot, by themselves, inhibit bacterial colonization.

Experimental composites containing antibacterial substances such as quaternary ammonium monomer (QAM) have thus been developed to provide an organic matrix that can effectively reduce bacterial growth by the release of cationic monomers [8,9]. QAM may inhibit biofilm formation since it increases bacterial cell permeability, leading to the disruption of the cell membrane wall and causing death [10,11].

Among QAMs, previous studies [12,13] have demonstrated high antibiofilm properties of DMADDM (2-(dimethylamino) ethyl methacrylate 1-bromododecane) and DMAHDM (2-(dimethylamino) ethyl methacrylate 1-bromohexadecane). The former has a 12-carbon chain and the latter a 16-carbon chain. Besides the chain length, increasing QAM concentration also improves the antibacterial effect of the composite [14,15]. Furthermore, incorporation of QAMs into restorative materials is promising since they are copolymerized with the composite, forming a network with its polymeric structure, thereby reducing leachability and maintaining the antibacterial properties for longer periods [16].

Although a significant reduction in *S. mutans* biofilm formation was described when these experimental composites were evaluated immediately after placement, after finishing and polishing, or after toothbrush abrasion [17], it is still unknown how this type of material can influence cariogenic demineralization at the enamel-composite margin. Therefore, the aim of this study was to investigate changes in enamel at the restorative material interface performed with experimental composites containing QAM after cariogenic challenge.

The research hypothesis was that the addition of a higher concentration of QAM in experimental composites influences changes in enamel at the interface (i) by maintaining the same initial hardness values of enamel-margin restorations, (ii) by resulting in minimal changes to the topography, and (iii) by reducing demineralization, as shown by micro-CT, after cariogenic challenge at the enamel-composite margin.

2. Material and methods

2.1. Synthesis of antibacterial monomers

Antimicrobial monomers were synthesized using the Menschutkin reaction, as previously reported [14]. In this addition reaction, a tertiary amine and an organic halide were added in equal amounts (60 mmol) to a round-bottom flask coupled to a condenser with 20 mL of ethanol and refluxed for 24 h. After that, the solvent was evaporated to dryness (rotary evaporator) to afford the pure monomer, which did not require any further purification. For each monomer, a different organic halide was used, since the tertiary amine was always 2-(dimethylamino)ethyl methacrylate (DMAEMA).

To characterize the reaction products, nuclear magnetic resonance (NMR) spectroscopy and high-resolution mass spectrometry (HRMS) were used. ^{1}H and ^{13}C NMR spectra were recorded on an Avance 200 MHz spectrometer (Bruker, Billerica, MA, USA) using $CDCl_3$ as solvent. Standard Bruker software was used throughout and chemical shifts were given in ppm (δ scale) and coupling constants (*J*) were given in hertz (Hz). High-resolution mass spectra were obtained on a Bruker microTOF II mass spectrometer using ESI.

2.1.1. Dimethylaminododecyl methacrylate (DMADDM)

Yield 24.07 g (98.8%); ^{1}H NMR ($CDCl_3$) δ 6.11 (s, 1H), 5.64 (s, 1H), 4.64 (br s, 2H), 4.11 (br s, 2H), 3.72–3.50 (m, 2H), 3.47 (s, 6H), 1.92 (s, 3H), 1.81–1.63 (m, 2H), 1.30–1.17 (m, 18H), 0.84 (t, $J = 6.6$ Hz, 3H); ^{13}C NMR ($CDCl_3$) δ 166.4, 135.3, 127.4, 65.6, 62.4, 58.3, 52.0, 32.0, 29.6, 29.5, 29.5, 29.4, 29.3, 26.4, 23.0, 22.7, 18.3, 14.2; HRMS-ESI: m/z $[M\text{-}Br]^+$ calculated for $C_{20}H_{40}NO_2Br$: 326.3059; found: 326.3062.

2.1.2. Dimethylaminohexadecyl methacrylate (DMAHDM)

Yield 27.52 g (99.3%); ^{1}H NMR ($CDCl_3$) δ 6.12 (s, 1H), 5.65 (s, 1H), 4.64 (br s, 2H), 4.13 (br s, 2H), 3.70–3.55 (m, 2H), 3.49 (s, 6H), 1.93 (s, 3H), 1.90–1.61 (m, 2H), 1.37–1.20 (m, 26H), 0.85 (t, $J = 5.7$ Hz, 3H); ^{13}C NMR ($CDCl_3$) δ 166.4, 135.3, 127.4, 65.6, 62.3, 58.3, 52.0, 32.0, 29.7, 29.6, 29.5, 29.4, 29.3, 26.4, 23.0, 22.7, 18.3, 14.2; HRMS-ESI: m/z $[M\text{-}Br]^+$ calculated for $C_{24}H_{48}NO_2Br$: 382.3685; found: 382.3691.

2.2. Formulation of experimental composites

Composite formulation was previously described by Rego et al. [17]. A mixture of bisphenol-A-glycidyl dimethacrylate (Bis-GMA) and triethylene glycol dimethacrylate (TEGDMA) (Esstech Inc., USA, batch 610-43) was used at a weight ratio of 50:50. This mixture was supplemented with 1% camphorquinone (Esstech Inc., USA; Lot TSNP004397) and 1% EDMAB amine (Sigma-Aldrich, MO, USA, lot MKBB3614), used as photoinitiator/co-initiator system. Pre-silanized spherical silica (average size of 7 nm; Aerosil R812, Evonik Degussa, lot 3523102) and pre-silanized SiO_2BaO particles (average size of 0.7 μm, Esstech Inc., USA, batch 699-17) were added at a total of 50% weight. QAMs (DMADDM or DMAHDM) were added at concentrations of 5% and 10% of the total organic matrix weight. The groups were named according to the alkyl chain length and monomer concentration, as follows: G12.5 (5% DMADDM), G12.10 (10% DMADDM), G16.5 (5% DMAHDM), G16.10 (10% DMAHDM), and control group (CG), without any QAM.

In addition, two more experimental groups: GZ250 and GIC, respectively a commercial composite (Z250, 3M Espe, Seefeld, Germany) and a commercial glass ionomer cement (Maxxion R, FGM, Santa Catarina, Brazil), were evaluated.

2.3. Enamel blocks and specimen preparation

Thirty-five enamel blocks (4 mm × 4 mm × 3 mm) were prepared from extracted bovine incisors, which had been previously stored in chloramine solution (pH 7.0) for 30 days at room temperature. One sample was cut from each crown using an ISOMET low-speed saw (Buehler, Lake Bluff, IL, USA) and two diamond discs (Extec Corp., Enfield, CT, USA), which were separated by a 4-mm diameter spacer. The enamel surface was ground flat with sandpaper discs (320, 600, and 1200 grades of Al_2O_3 papers; Buehler, Lake Bluff, IL, USA) and polished with felt paper soaked in diamond slurry (1 μm; Buehler). This procedure resulted in removal of about 100 μm of enamel. Microhardness was determined by performing five indentations in randomized areas at the enamel surface (Knoop hardness diamond, 25 g, 5 s, HMV-2000; Shimadzu Corporation, Tokyo, Japan). Only enamel specimens with hardness values ranging from 320 to 385 KHN were selected.

After enamel block selection, standardized cavities (1.5 mm diameter for 1.5 mm deep) were prepared at the center of the enamel surface using a spherical diamond bur # 2292 (KG Sorensen, Barueri, SP, Brazil). Specimens were randomly distributed into seven groups (n = 5). In all groups, except in group GIC, enamel and dentin were etched with 35% phosphoric acid (3M ESPE, St Paul, MN, USA) for 15 s, rinsed off for 15 s, and blot-dried. Thereafter, the adhesive system (Adper Single Bond 2, 3M ESPE, St Paul, MN, USA) was applied in two coats with a microbrush tip, lightly dried, and photocured for 10 s following the manufacturer's instructions.

Restorative materials were inserted in the prepared cavity and covered with a polyester strip and a glass slab under pressure to remove excess material from the cavity. For light-cured composites, polymerization was carried out through the polyester strip for 40 s using a light-curing unit (Radii CALL, SDI) with a power density of 800 mW/cm^2.

After 7 days of storage at 4 °C at a relative humidity of 100%, to obtain reference surfaces for lesion depth determination, the restoration surfaces were ground flat as described above. Then, the initial enamel surface microhardness (SMH) (distance of 50 mm from the restoration margin) was measured (Knoop indentation at 50 g, 15 s with five indentations, 100 mm from each other). After that, half of the restoration and enamel margins were covered by two layers of nail varnish for maintenance of a sound surface reference [18].

2.4. Biofilm formation

The biofilm model chosen for the experiment was composed of *S. mutans*. This microorganism plays the main role in the onset and progression of enamel caries and it is commonly found in the oral cavity.

The specimens were sterilized with ethylene oxide and fixed at the bottom of well plates (24-well plate) with a resistant acid varnish. *S. mutans* isolate from the American Type Culture Collection (ATCC 25175, Fundação Oswaldo Cruz, Rio de Janeiro, RJ, Brazil) was cultured in brain heart infusion (BHI) (Difco, Sparks, USA) broth supplemented with 2% sucrose at 37 °C under anaerobic conditions for 24 h. Afterwards, the bacterial suspension was adjusted to an optical density of 0.5 at 550 nm using a UV/Vis spectrophotometer (Beckman Coulter DU® 530, LifeScience, San Diego, CA, USA) in accordance with the McFarland scale (Biomérieux Brazil S.A., RJ, Brazil). The suspension was diluted 1:100 and 10 μL of this suspension was added to each well, containing a specimen with 2 mL of BHI broth supplemented with 2% sucrose. The 24-well plates were kept for 48 h at 37 °C under microaerophilic conditions. During the experiment, the growth medium was changed every 24 h.

2.5. Knoop microhardness analysis

After the biofilm formation period, enamel samples were removed from the plates and the nail varnish on the reference surfaces was carefully removed with acetone-soaked cotton wool. The final surface microhardness evaluation (SMH1) was performed at 100 μm apart from the initial indentations on the enamel and restoration. The percentage of hardness change for enamel and restorative materials was calculated as follows:

$$\%\text{hardness} = 100(\text{SMH1} - \text{SMH})/\text{SMH}.$$

2.6. 3D non-contact profilometry

To perform 3D non-contact profilometry, the specimen with microhardness values more similar to the mean values of each group was selected. The surface topography of the specimens was analyzed by a 3D profilometer (Nanovea PS50 Optical, NANOVEA Inc., Irvine, USA). The measurements were performed with a chromatic confocal sensor with a white light axial source at a scan velocity of 3 mm/s and with a refractive index of 1 [19].

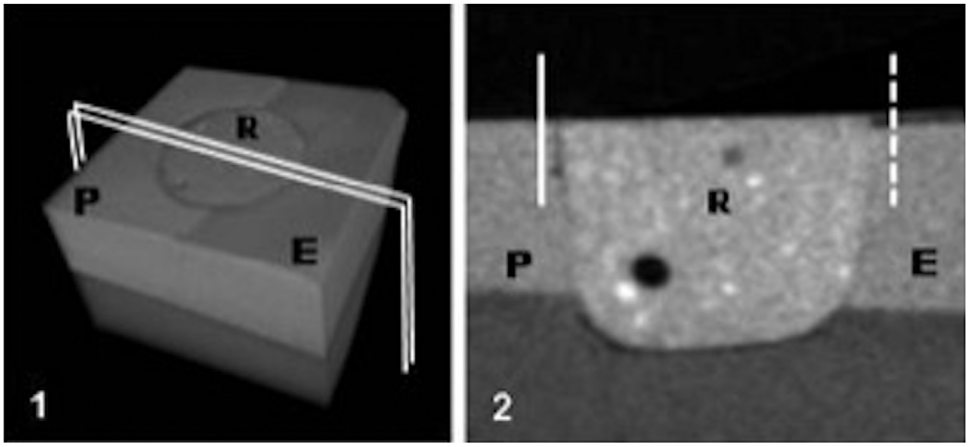

Fig. 1 – Left (1): micro-CT tridimensional specimen visualization for quantification of mineral density in sound (P – protected enamel area), carious exposed enamel (E – exposed enamel area), and restoration (R – restorative material). White lines indicated the direction of reslicing. Right (2): representative micro-CT slice. Full and dotted lines indicate the area where the gray values were measured (P – protected enamel area; E – enamel exposed to the biofilm).

2.7. *Micro-CT acquisition, reconstruction, and analysis*

The specimens were scanned using micro-CT following the methodology described by Neves et al. [20]. A high-energy micro-CT scanner (Skyscan 1173, Bruker, Kontich, Belgium) was used, with the following acquisition parameters: 70 kV, 114 μA, 14.6 μm pixel size, 260 ms exposure, frame averaging of 5, and rotation step of 0.5° through 360°. A flat-field reference image was obtained before the first scan and the random-movement amplitude was set to 20 lines to reduce ring artifacts. A 1-mm aluminum filter was also used to reduce the beam hardening effect. The data were saved as 16-bit TIFF format projections.

The acquired micro-CT projections were reconstructed into cross-sectional slices using the Nrecon v.1.6.6 software interface (Bruker). Specific reconstruction settings included a 50% beam hardening correction, ring artifact correction factor of 5, and input of optimal contrast limits (0–0.075) for all stack reconstructions. The reconstructed slices were saved in 8-bit BMP format. A volume of interest (VOI) was then cropped from the original stacks and aligned, with the protected enamel side on the left side, exposed enamel side on the right side, and the restored cavity at the center (Fig. 1.1).

After that, 10 representative slices were chosen from the VOI and line profiles were taken from the enamel surface to at least half of the enamel layer depth near the interface in both the protected (sound) and exposed (carious) areas (Fig. 1.2). The sound and carious profiles were compared and the integrated difference in gray values were measured and taken as the representative mineral change. Negative values indicate net mineral loss, while positive values indicate mineral density increase. Lesion depth was also obtained from all evaluated samples.

2.8. *Statistical analysis*

Microhardness values were analyzed using SPSS for Windows, version 20.0 (IBM Corporation, New York, NY, USA), in order to calculate correlations between groups and the percentage of surface microhardness loss (SMH%). Results were first subjected to the Shapiro–Wilk and Levene's tests to evaluate the data distribution model. The Kruskal–Wallis, Mann–Whitney, and Tukey's HSD test were carried out to compare the microhardness values according to the groups and distances between the enamel-restoration margin. Tukey's HSD test was used for the micro-CT analysis. The significance level was set at 5%. A descriptive analysis was used for 3D profilometry.

3. Results

3.1. *Surface microhardness loss*

After the cariogenic challenge, a decrease in surface microhardness was observed on the enamel near the restorative interface in all groups evaluated, with a significant effect for the restorative material (Table 1). However, this was not observed for the distance from the margin (Kruskal–Wallis test, $p > 0.05$) (Fig. 2). Overall, specimens restored with glass ionomer cement (GIC) presented statistically significant higher microhardness values (resistance to demineralization) compared to the other materials for all indentation distances.

The Mann–Whitney test was used to detect differences in total mineral loss among the groups. Overall, significant high mineral loss was observed for all groups; however, G16.10 presented better resistance to mineral loss among the other composites. In addition, GIC had statistically lower mineral loss compared to the other groups (Fig. 3, Table 1).

Tukey's HSD test was used to evaluate whether there were statistical differences among the different groups at the same indentation distance from the enamel margin. All GIC indentation distances had statistical differences among the other groups (Table 1).

Table 1 – Percentage of hardness loss for enamel adjacent to restorative materials after biofilm formation at different distances.

Distance	Hardness loss % (SD)						
	G12.5	G12.10	G16.5	G16.10	CG	GZ250	GIC
50 μm	88.5 (3.01)^{A}	90.4 (1.56)^{A}	92.5 (0.44)^{A}	78.6 (5.20)^{A}	92.4 (0.89)^{A}	92.8 (0.47)^{A}	27.5 (14.29)^{B}
150 μm	88.4 (3.01)^{A}	87.1 (3.25)^{A}	93.0 (0.35)^{A}	79.5 (3.60)^{A}	92.5 (1.14)^{A}	92.9 (0.59)^{A}	24.2 (8.64)^{B}
250 μm	85.1 (3.48)^{A}	84.7 (3.89)^{A}	92.2 (0.47)^{A}	78.6 (4.23)^{A}	89.9 (2.50)^{A}	92.9 (0.43)^{A}	16.5 (10.57)^{B}
350 μm	84.3 (3.43)^{A}	84.7 (3.32)^{A}	92.1 (1.61)^{A}	78.2 (4.82)^{A}	88.6 (3.38)^{A}	92.5 (0.52)^{A}	22.5 (11.03)^{B}
450 μm	85.1 (2.77)^{A}	80.8 (2.84)^{A}	91.1 (1.52)^{A}	77.4 (4.13)^{A}	87.9 (2.79)^{A}	91.5 (1.04)^{A}	24.6 (9.76)^{B}

Different letters indicate statistically significant differences ($p < 0.05$).

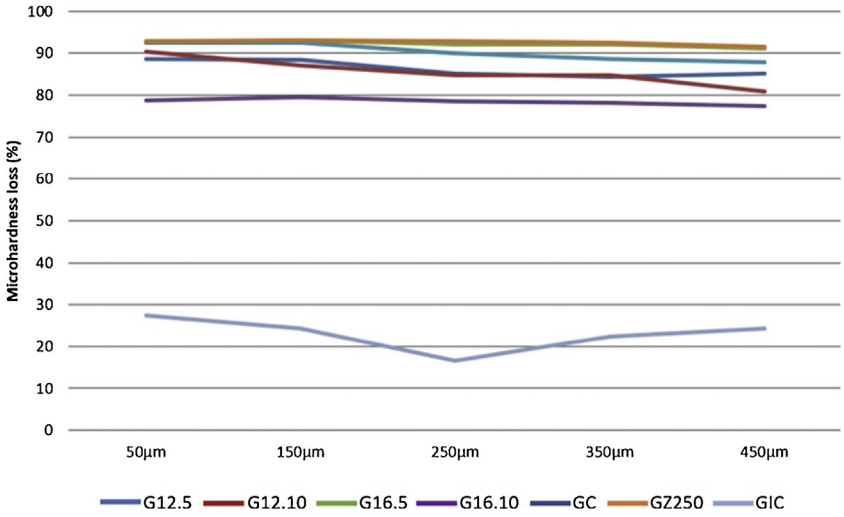

Fig. 2 – Mean percentage of surface microhardness loss at the enamel margin according to the distance from the restorative interface after cariogenic challenge.

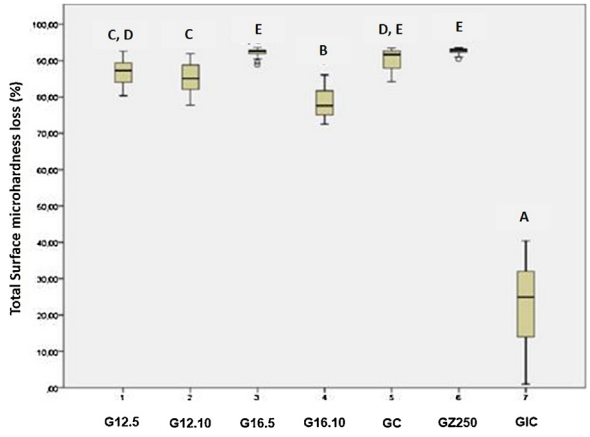

Fig. 3 – Percentage of total surface microhardness loss for enamel adjacent to restorative materials after biofilm formation, regardless of the distance from the restoration. Different letters indicate statistically significant differences ($p < 0.05$, Mann–Whitney test).

3.2. *3D non-contact profilometry and micro-CT analysis*

Table 2 shows linear surface roughness values (Ra), volumetric surface roughness (Sa), and the step (gap) between the covered and exposed area for each group. GIC presented lower step sizes and linear surface roughness values. Regarding Sa, G16.10 resulted in rougher surfaces compared to all groups evaluated.

Table 2 – Mean surface roughness in μm (Ra and Sa) and gap between protected and exposed enamel areas.

	Ra	Sa	Gap
G12.5	−0.14	−0.22	10.22
G12.10	−0.16	−0.20	10.69
G16.5	−0.03	−0.24	7.97
G16.10	−0.22	0.12	6.77
CG	−0.01	−0.39	12.5
GZ250	−0.45	−0.38	5.32
GIC	−0.92	−1.20	4.88

Fig. 4 shows profilometry images of surface roughness after the cariogenic challenge. Note that all groups presented differences in roughness between the protected area and the exposed enamel, resulting in a step between the two areas.

Fig. 5 shows mineral density changes (represented by differences in gray values) in enamel adjacent to the restorations measured by micro-CT. All specimens presented a reduction in mineral density (higher absolute values indicate greater mineral loss), except for the GIC group, which exhibited a mineral density increase after the cariogenic challenge. Table 3 shows values of lesion depth among the groups. Although both GC

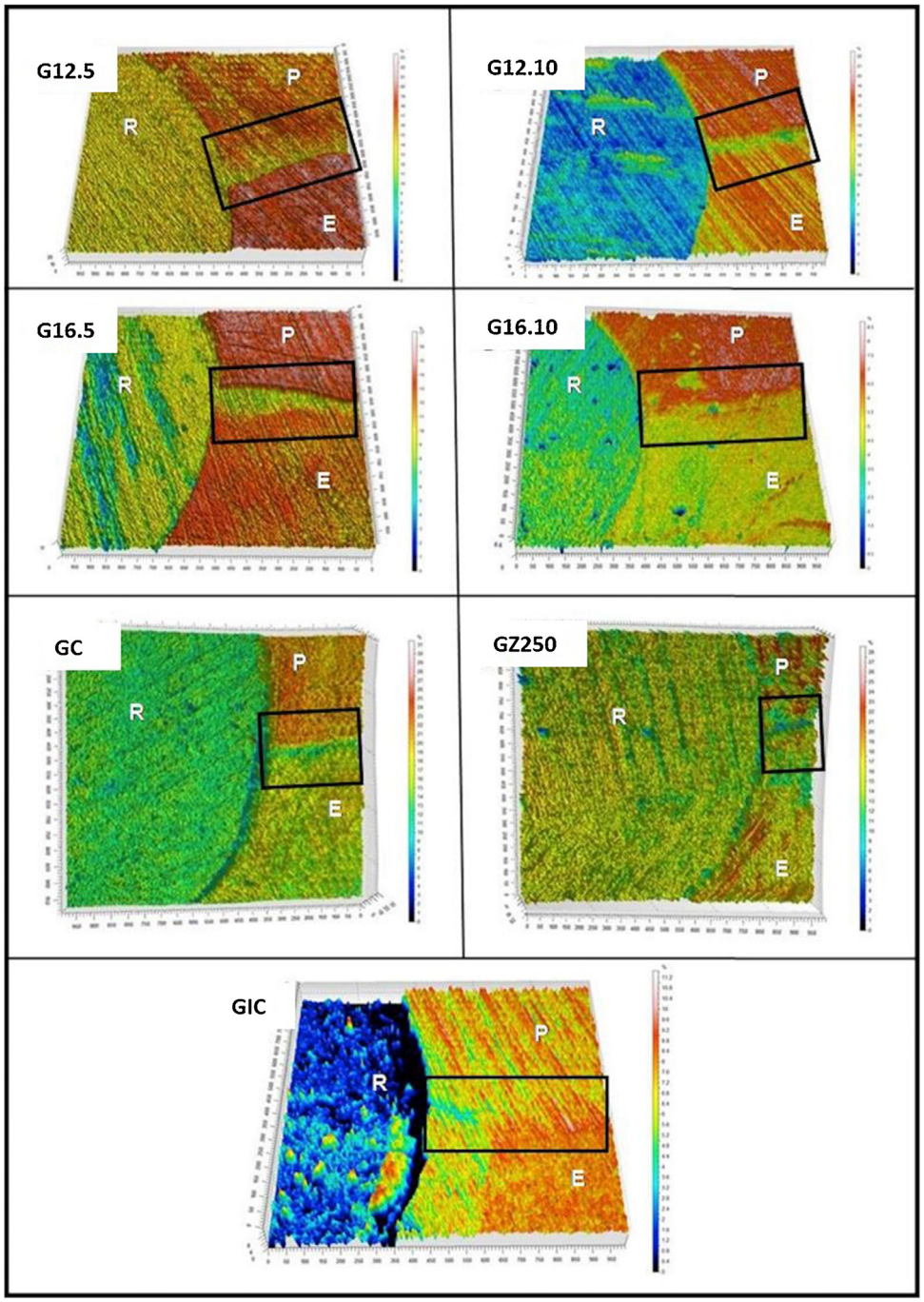

Fig. 4 – 3D profilometry surface image representation of the interface between the tooth and the restorative material (R) after the cariogenic challenge; protected (P) and exposed (E) enamel. Full black line rectangles indicate the analyzed areas.

and GZ250 showed higher lesion depths, values were not statistically significant from the other groups.

4. Discussion

Even with all advances in dental materials research, replacement of composite restorations due to recurrent caries is still common [21]. In this regard, incorporation of antibacterial monomers into dental composites seems to be a promising alternative for inhibiting biofilm formation and decreasing acid production by microorganisms [16]. This is the first study to investigate demineralization of the enamel adjacent to restoration margins in cavities filled with experimental composites containing QAMs subjected to a cariogenic challenge.

Regarding the complex degradation of the dental structure when subjected to a cariogenic challenge, it has been shown that the Knoop hardness test is a pertinent method to confirm demineralization after acid challenges [18]. This test was used in the present study to verify whether restorative materials with reported antimicrobial properties [17] can protect

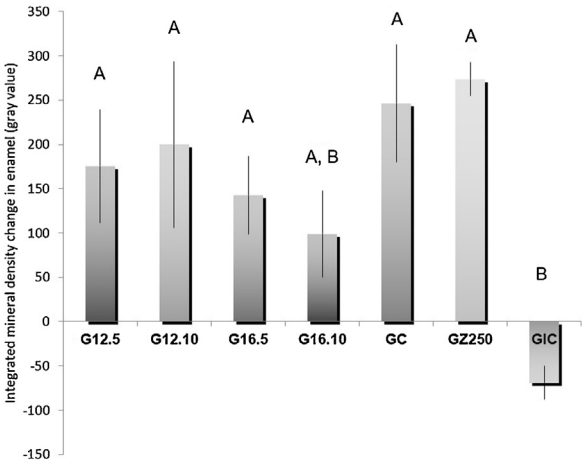

Fig. 5 – Mean gray values indicate mineral loss in adjacent enamel restorations. Different letters indicate statistically significant differences ($p < 0.05$) (Tukey's HSD test).

Table 3 – Mean ± standard deviation of lesion depth (μm) among the groups*.

Groups	Lesion depth
G12.5	142.3 ± 18.4[a]
G12.10	146.0 ± 11.9[a]
G16.5	148.6 ± 13.9[a]
G16.10	142.3 ± 21.9[a]
GC	149.6 ± 7.3[a]
GZ250	160.6 ± 20.6[a]

Different letters indicate statistically significant differences ($p < 0.05$) (Tukey's HSD test).

* As lesions in GIC group showed increase in integrated mineral loss, no measurable depth of lesion could be measured.

the enamel at the interface against demineralization induced by cariogenic biofilm formation. Compared to the controls (CG and GZ250), only the experimental composites with 10% quaternary ammonium were able to reduce total hardness loss (Fig. 3). On the other hand, the adjacent enamel in cavities restored with G16.10 (10% DMAHDM) presented the lowest microhardness percentage loss among the experimental composites. In accordance with the current literature, DMAHDM has the longest alkyl chain [22], which is more effectively associated with the inhibitory potential of *S. mutans* growth [13,22]. In the present study, when the concentration of DMAHDM was 10%, there might have been lower biofilm formation, which culminated in lower demineralization percentage around the enamel-restoration margin.

The short-chain quaternary monomer DMADDM has also shown efficiency in inhibiting biofilm growth [15,16,23,24]. In line with that, our results indicated less demineralization on the margins of cavities restored with DMADDM at 5% and 10% concentrations when compared to commercial composite GZ250 (Fig. 3). However, unlike the concentration of DMAHDM, that of DMADDM in experimental composite did not influence the prevention of enamel demineralization around restoration margins.

In the present study, commercial composite GZ250 served as reference and a negative control while GIC was used as a positive control as its ability to interact with dental hard tissues is widely known [25–27]. The fluoride-releasing GIC materials exhibit a secondary caries inhibiting effect even during cariogenic challenge [28]. However, the concentration of ions released appeared not sufficient to inhibit bacterial growth [29]. This ionic diffusion capacity certainly promoted remineralization of the exposed enamel, as seen in the profilometry (Table 2 and Fig. 4) and micro-CT analyses (Fig. 5), resulting in fewer alterations in microhardness values.

A significant difference was found in the percentage of surface microhardness change in adjacent restorations between the CG and commercial composite GZ250. In general, the CG presented better results compared to the commercial material and, even though none of them had an antibacterial monomer in their composition, filler sizes could be a reasonable explanation for these findings. Whereas the control group was made up of a standardized filler size of 40 nm, the commercial composite, according to the manufacturers, contained filler sizes that could reach up to 3.5 μm. It is known that after polishing, fillers could come off the matrix, leading to a rougher and porous surface, facilitating the growth of *S. mutans* and biofilm formation [30,31].

The present study did not demonstrate any statistical difference in enamel demineralization at different distances from the restoration margins. Glasspoole et al. [32] observed that GICs were able to influence mineral changes in enamel up to 800 μm from the restoration margin. Thus, one can speculate that the area of protection of the different materials in the present study might be even higher than 450 μm, which was the indentation farthest from the margin used in our experiment.

Surface roughness was evaluated by 3D non-contact profilometry. By measuring enamel loss with a laser, this method does not damage the specimen's surface as occurs in contact profilometry [33]. In addition, this method enables a volumetric loss analysis by the surface place generated [34,35]. Higher linear surface roughness was found in the CG and lower volumetric surface roughness and step sizes were found in the GIC group. This result was similar to those observed in the microhardness test and in the micro-CT analysis, which means that rougher surfaces were found in groups without any antimicrobial monomer. By contrast, GIC produced protective properties against demineralization [35] and resulted in fewer surface modifications.

A micro-CT analysis is more advantageous than the conventional microradiographic technique for the study of demineralization since it allows a volumetric and non-destructive analysis of the whole specimen [36]. In all experimental groups, a decrease in mineral content was detected while comparing the sound area with the area exposed to the biofilm. The micro-CT analysis corroborated the results observed in the microhardness test, which demonstrated that G16.10 exhibited less mineral loss. Among all restoration groups, GIC was the only group with an increase in mineral density. This result may be attributed to the well-known ability of GICs to release fluoride ions constantly and to their diffusion through the substrate, enabling a positive mineral change [7]. Additionally, our cariogenic challenge (biofilm formation model) could be considered short (48 h), i.e., with the presence of acids only for a short period. This might have

facilitated fluoride ion release from the GIC to the restoration margins without further mineral loss.

Although the development of primary or recurrent dental caries depends on a complex microbial community, we used bacterial monocultures to cariogenic challenge [17]. Nevertheless, this biofilm model was appropriate for the posed research question, considering the need to better understand the results obtained with single-species models and experimental composites containing quaternary ammonium monomers.

Despite evaluating the demineralization protection capacity of DMADDM and DMAHDM for the first time, this study could not address all the complexity of the *in vivo* caries formation process. Furthermore, with the results obtained, we refute hypothesis (i), since all experimental composites presented lower microhardness values. However, hypotheses (ii) and (iii) could be partially accepted, since the addition of 10% DMAHDM produced lower changes in the topography and lower demineralization, confirmed by micro-CT. Thus, in addition to the antibiofilm properties already demonstrated in previous studies [17], in general, QAMs were able to prevent demineralization around enamel-restoration margins after the cariogenic challenge.

5. Conclusion

Except for 5% DMAHDM, all experimental composites demonstrated a statistically significant reduction in demineralization around the enamel-restoration margins. DMAHDM at 10% concentration presented better resistance to the cariogenic challenge. Furthermore, enamel at the margins of the GIC restoration had a remineralization behavior.

In general, the addition of antibacterial monomers, based on QAMs, to experimental composites improved resistance to demineralization in enamel-restoration margins when subjected to cariogenic challenge.

REFERENCES

[1] Li Y, Carrera C, Chen R, Li J, Lenton P, Rudney JD, et al. Degradation in the dentin-composite interface subjected to multi-species biofilm challenges. Acta Biomater 2014;0:375–83.

[2] Chen MH. Update on dental nanocomposites. J Dent Res 2010;6:549–60.

[3] Ferracane JL. Resin composite—state of the art. Dent Mater 2011;27:29–38.

[4] Spencer P, Ye Q, Misra A, Goncalves SE, Laurence JS. Proteins, pathogens, and failure at the composite-tooth interface. J Dent Res 2014;93:243–9.

[5] Loesche WJ. Role of *Streptococcus mutans* in human dental decay. Microbiol Rev 1986;50:353–80.

[6] Totiam P, González-Cabezas C, Fontana MR, Zero DT. A new in vitro model to study the relationship of gap size and secondary caries. Caries Res 2007;41:467–73.

[7] Cenci MS, Pereira-Cenci T, Cury JA, Ten Cate JM. Relationship between gap size and dentine secondary caries formation assessed in a microcosm biofilm model. Caries Res 2009;43:97–102.

[8] Cheng L, Zhang K, Melo MA, Weir MD, Zhou X, Xu HH. Anti-biofilm dentin primer with quaternary ammonium and silver nanoparticles. J Dent Res 2012;91:598–604.

[9] Li F, Weir MD, Chen J, Xu HH. Comparison of quaternary ammonium-containing with nano-silver-containing adhesive in antibacterial properties and cytotoxicity. Dent Mater 2013;29:450–61.

[10] Namba N, Yoshida Y, Nagaoka N, Takashima S, Matsuura-Yoshimoto K, Maeda H, et al. Antibacterial effect of bactericide immobilized in resin matrix. Dent Mater 2009;25:424–30.

[11] Beyth N, Yudovin-Farber I, Bahir R, Domb AJ, Weiss EI. Antibacterial activity of dental composites containing quaternary ammonium polyethylenimine nanoparticles against *Streptococcus mutans*. Biomaterials 2006;27:3995–4002.

[12] Li F, Weir MD, Xu HH. Effects of quaternary ammonium chain length on antibacterial bonding agents. J Dent Res 2013;92:932–8.

[13] Zhou H, Li F, Weir MD, Xu HH. Dental plaque microcosm response to bonding agents containing quaternary ammonium methacrylates with different chain lengths and charge densities. J Dent 2013;41:1122–31.

[14] Liang X, Söderling E, Liu F, He J, Lassila LV, Vallittu PK. Optimizing the concentration of quaternary ammonium dimethacrylate monomer in bis-GMA/TEGDMA dental resin system for antibacterial activity and mechanical properties. J Mater Sci Mater Med 2014;25:1387–93.

[15] Cheng L, Weir MD, Zhang K, Arola DD, Zhou X, Xu HH. Dental primer and adhesive containing a new antibacterial quaternary ammonium monomer dimethylaminododecyl methacrylate. J Dent 2013;41:345–55.

[16] Zhang K, Cheng L, Wu EJ, Weir MD, Bai Y, Xu HH. Effect of water ageing on dentin bond strength and anti-biofilm activity of bonding agents containing new monomer dimethylaminododecyl methacrylate. J Dent 2013;41:504–13.

[17] Rego GF, Vidal ML, Viana GM, Cabral LM, Schneider LFJ, Portela MB, et al. Antibiofilm properties of model composites containing quaternary ammonium methacrylates after surface texture modification. Dent Mater 2017;33:1149–56.

[18] Salas CF, Guglielmi CA, Raggio DP, Mendes FM. Mineral loss on adjacent enamel glass ionomer cements restorations after cariogenic and erosive challenges. Arch Oral Biol 2011;56:1014–9.

[19] Gong SQ, Niu LN, Kemp LK, Ryou H, Qi YP, Blizzard JD, et al. Quaternary ammonium silane-functionalized methacrylate resin composition with antimicrobial activities and self-repair potential. Acta Biomater 2012;8:3270–82.

[20] Neves AA, Lourenço RA, Alves HD, Lopes RT, Primo LG. Caries-removal effectiveness of a papain-based chemo-mechanical agent: a quantitative micro-CT study. Scanning 2015;37:258–64.

[21] Cheng L, Zhang K, Weir MD, Liu H, Zhou X, Xu HH. Effects of antibacterial primers with quaternary ammonium and nano-silver on *Streptococcus mutans* impregnated in human dentin blocks. Dent Mater 2013;29:462–72.

[22] Li F, Weir MD, Chen J, Xu HH. Effect of charge density of bonding agent containing a new quaternary ammonium methacrylate on antibacterial and bonding properties. Dent Mater 2014;30:433–41.

[23] He J, Söderling E, Österblad M, Vallittu PK, Lassila LV. Synthesis of methacrylate monomers with antibacterial effects against *S. mutans*. Molecules 2011;16:9755–63.

[24] Chen C, Weir MD, Cheng L, Lin NJ, Lin-Gibson S, Chow LC, et al. Antibacterial activity and ion release of bonding agent containing amorphous calcium phosphate nanoparticles. Dent Mater 2014;30:891–901.

[25] Fúcio SB, Paula AB, Sardi JC, Duque C, Correr-Sobrinho L, Puppin-Rontani RM. *Streptococcus mutans* biofilm influences on the antimicrobial properties of glass ionomer cements. Braz Dent J 2016;27:681–7.
[26] Forss H, Seppa L. Studies on the effect of fluoride released by glass ionomers in the oral cavity. Adv Dent Res 1995;9:389–93.
[27] Wiegand A, Buchalla W, Attin T. Review on fluoride releasing restorative materials fluoride release and uptake characteristics, antibacterial activity and influence on caries formation. Dent Mater 2007;23:343–62.
[28] Krämer N, Schmidt M, Lücker S, Domann E, Frankenberger R. Glass ionomer cement inhibits secondary caries in an in vitro biofilm model. Clin Oral Invest 2018;22:1019–31.
[29] Yoshihara K, Nagaoka N, Maruo Y, Sano H, Yoshida Y, Van Meerbeek B. Bacterial adhesion not inhibited by ion-releasing bioactive glass filler. Dent Mater 2017;33:723–34.
[30] Park JW, Song CW, Jung JH, Ahn SJ, Ferracane JL. The effects of surface roughness of composite resin on biofilm formation of *Streptococcus mutans* in the presence of saliva. Oper Dent 2012;37:532–9.
[31] Ionescu A, Wutscher E, Brambilla E, Schneider-Feyrer S, Giessibl FJ, Hahnel S. Influence of surface properties of resin-based composites on in vitro *Streptococcus mutans* biofilm development. Eur J Oral Sci 2012;120:458–65.
[32] Glasspoole EA, Erickson RL, Davidson CL. Demineralization of enamel in relation to the fluoride release of materials. Am J Dent 2001;14:8–12.
[33] Heurich E, Beyer M, Jandt KD, Reichert J, Herold V, et al. Quantification of dental erosion a comparison of stylus profilometry and confocal laser scanning microscopy (CLSM). Dent Mater 2010;26:326–36.
[34] Rodriguez JM, Bartlett DW. A comparison of two-dimensional and three-dimensional measurements of wear in a laboratory investigation. Dent Mater 2010;26:e221–5.
[35] Paepegaey AM, Barker ML, Bartlett DW, Mistry M, West NX, Hellin N, et al. Measuring enamel erosion: a comparative study of contact profilometry, non-contact profilometry and confocal laser scanning microscopy. Dent Mater 2013;29:1265–72.
[36] Zou W, Gao J, Jones AS, Hunter N, Swain MV. Characterization of a novel calibration method for mineral density determination of dentine by X-ray micro-tomography. Analyst 2009;134:72–9.